Food and Chemical Toxicology 128 (2019) 129–136

Contents lists available at ScienceDirect

Food and Chemical Toxicology

journal homepage: www.elsevier.com/locate/foodchemtox

Antioxidant effects of sulforaphane in human HepG2 cells and immortalised hepatocytes

Peng Liu[a], Wei Wang[a], Jonathan Tang[a], Richard P. Bowater[b], Yongping Bao[a,*]

[a] Norwich Medical School, University of East Anglia, Norwich Research Park, Norwich, Norfolk, United Kingdom
[b] School of Biological Sciences, University of East Anglia, Norwich Research Park, Norwich, Norfolk, United Kingdom

ARTICLE INFO

Keywords:
Sulforaphane
Hepatocyte
Nrf2
GSH
Oxidative stress
Chemopreventive

ABSTRACT

Sulforaphane (SFN) has shown anti-cancer effects in cellular and animal studies but its effectiveness has been limited in human studies. Here, the effects of SFN were measured in both human hepatocytes (HHL5) and hepatoma (HepG2) cells. Results showed that SFN inhibited cell viability and induced DNA strand breaks at high doses (≥ 20 μM). It also activated the nuclear factor (erythroid-derived 2)-like 2 (Nrf2), and increased intracellular glutathione (GSH) levels at 24 h. Pre-treatment with a low dose SFN (≤ 5 μM) protected against hydrogen peroxide (H_2O_2)-induced cell damage. High doses of SFN were more toxic towards HHL5 compared to HepG2 cells; the difference is likely due to the disparity in the responses of Nrf2-driven enzymes and -GSH levels between the two cell lines. In addition, HepG2 cells hijacked the cytoprotective effect of SFN over a wider dose range (1.25–20 μM) compared to HHL5. Manipulation of levels of GSH and Nrf2 in HepG2 cells confirmed that both molecules mediate the protective effects of SFN against H_2O_2. The non-specific nature of SFN in the regulation of cell death and survival could present undesirable risks, i.e. be more toxic to normal cells, and cause chemo-resistance in tumor cells. These issues should be addressed in the context for cancer prevention and treatment before large scale clinical trials are undertaken.

1. Introduction

Isothiocyanates, found in cruciferous vegetables, have been identified as chemopreventive phytochemicals. One of the most important dietary isothiocyanates is sulforaphane (1-isothiocyanate-(4R)-(methylsulfinyl) butane, SFN), first isolated from broccoli in 1992 (Zhang et al., 1992). SFN is derived from glucoraphanin (4-methylsulfinylbutyl glucosinolate), and is abundant in both broccoli and broccoli sprouts (Nakagawa et al., 2006). The cytoprotective effect of SFN comes largely from the activation of nuclear factor (erythroid-derived 2)-like 2 (Nrf2), a master regulator involved in cell redox homeostasis and stress adaptation (Baird and Dinkova-Kostova, 2011). Under basal conditions, Nrf2 is sequestered in the cytoplasm by redox-sensitive Kelch-like ECH-associated protein 1 (Keap1), which associates with Cul3 and brings Nrf2 in close proximity to Cul3-based E3 ligase complex so Nrf2 degrades via the ubiquitin-26S proteasomal pathway (Zhang et al., 2005). With a half-life of around 20 min (Katoh et al., 2005), Nrf2 is normally maintained at a low cellular level. The interaction of SFN with Keap1 disrupts this function and allows nuclear accumulation of Nrf2. Although there are conflicting *in vitro* and *in vivo* data regarding which cysteine residues react with SFN, evidence showed that modification of C151 is essential for its action (Hu et al., 2011). Nrf2 then binds to the antioxidant responsive element (ARE) and enhances the transcription of more than 200 target genes, many of which provoke strong cytoprotective responses. Of significance is that Nrf2 controls the production, utilization and regeneration of glutathione (GSH), the most abundant antioxidant cofactor within cells (Townsend et al., 2003), by regulating the rate-limiting enzyme for GSH synthesis, Glutamate cysteine ligase (GCL, previous known as glutamylcysteine synthetase, γ-GCS) (Lu, 2009), reactive oxygen species (ROS)-detoxifying enzymes such as glutathione transferase (GST) (Thimmulappa et al., 2002), and NADPH-generating enzymes (Mitsuishi et al., 2012).

In addition to the cytoprotective effect, SFN has also been shown to exhibit cytotoxic effects including promoting ER stress and cell death (Moon et al., 2010; Liu et al., 2017; Chung et al., 2015); disrupting mitochondria (Tang and Zhang, 2005), tubulin and microtubule function (Jackson and Singletary, 2004; Jackson et al., 2007; Byun et al., 2016); inducing DNA damage (Sestili et al., 2010), apoptosis and cell cycle arrest (Pham et al., 2004; Gamet-Payrastre et al., 2000; Suppipat et al., 2012; Park et al., 2014); inhibiting telomerase activity (Moon

* Corresponding author. Bob Champion Research and Education Building, James Watson Road, University of East Anglia, Norwich Research Park, Norwich, NR4 7UQ, UK.
E-mail address: Y.Bao@uea.ac.uk (Y. Bao).

https://doi.org/10.1016/j.fct.2019.03.050
Received 17 December 2018; Received in revised form 20 March 2019; Accepted 26 March 2019
Available online 30 March 2019

et al., 2010; Herz et al., 2014) and protein-protein interaction in Hsp90 complex (Li et al., 2012a). The complex bioactivities of SFN and subsequent cellular responses are highly dependent upon the dose and duration of SFN treatment. Therefore, understanding of the effects of SFN in non-cancerous and cancerous cells has great importance in cancer management.

An effective cancer therapy requires high selectivity towards cancer cells. Comparisons of results of SFN bioactivities on normal and cancerous cells have been inconsistent. Several normal epithelial cell lines are relatively resistant to apoptosis induction by SFN at concentrations that are lethal to cancer cells (Pledgie-Tracy et al., 2007; Clarke et al., 2011). Zeng et al. reported SFN activated survival signalling in non-tumorigenic NCM460 colon cells but activated apoptotic signalling in tumorigenic HCT116 colon cells, and that may play a critical role in the higher potential of SFN to inhibit cell proliferation in colon cancer cells than in normal colon cells (Zeng et al., 2013). The transcription factor specificity protein 1 was linked to SFN-induced prostate cancer specific cytotoxicity (Beaver et al., 2014). Conversely, SFN was more cytotoxic to lymphoblastoid than to leukaemia cells (Misiewicz et al., 2007). The effects of SFN on non-transformed T-lymphocytes were similar to those recorded on Jurkat T-leukaemia cells (Fimognari et al., 2004). SFN showed broad and complex effects on DNA methylation profiles in both normal and cancerous prostate epithelial cells (Wong et al., 2014) and regulated the Nrf2/ARE signalling pathway differently in human untransformed epithelial colon cells when compared to colorectal cancer cells (Lubelska et al., 2016; Wang et al., 2015a). Negrette-Guzman et al. demonstrated SFN modulates mitochondrial dynamics differentially in normal and cancer cells (Negrette-Guzman et al., 2017). The transcriptional response to SFN on cell cycle related genes was dependent on the cell line and presumably the state of cancer progression (Constantinescu et al., 2014; Agyeman et al., 2012). However, to date, an understanding of why SFN has any specificity remains elusive.

The aim of this study was to compare the cytotoxic and cytoprotective effects of SFN in a human hepatoma cell line, HepG2, and in an immortalised human hepatocyte-derived cell line, HHL5 (Clayton et al, 2005), thereby providing evidence on the possible dual role of SFN in cancer biology.

2. Experimental methods

2.1. Materials

SFN was purchased from Toronto Research Chemicals (Canada). 3-(4,5-Dimethyilthiazol-2-yl)-2,5-diphenyltetrayolium bromide (MTT), dimethyl sulfoxide (DMSO), hydrogen peroxide (H_2O_2), DL-Buthionine sulfoximine (BSO), and Bradford reagent were all purchased from Sigma-Aldrich (Dorset, UK). Complete protease inhibitors were obtained from Roche Applied Science (West Sussex, UK). Primary antibodies to Nrf2, GCS, catalase (CAT), superoxide dismutase-1 (SOD-1), heme oxygenase-1 (HO-1), NAD(P)H: quinone oxidoreductase (NQO1), glutathione peroxidase 4 (GPX4), Sam68, β-actin, HRP-conjugated goat anti-rabbit and rabbit anti-goat IgG were all purchased from Santa Cruz Biotechnology (Santa Cruz, Germany). Primary antibody to phospho-Chk2 (Thr68) was purchased from Cell Signalling (Hitchin, UK). The siRNAs for Nrf2 (target sequence, 5′-CCCATTGATGTTTCTGATCTA-3′) and AllStars Negative Control siRNA were purchased from Qiagen (West Sussex, UK). Electrophoresis and western blotting supplies were obtained from Bio-Rad (Hertfordshire, UK), and the chemiluminescence kit was from GE Healthcare (Little Chalfont, UK).

2.2. Cell culture

Immortalised human hepatocytes, defined as HHL5 and HepG2 cells were cultured in Dulbecco's Modified Eagle's Medium (DMEM, Gibco) containing 4.5 g/l D-glucose and Non-Essential Amino Acids, supplemented with 10% heat-inactivated foetal bovine serum (FBS, Invitrogen), 1% L-glutamine (200 mM, Gibco), antibiotics (penicillin 100 U/ml and streptomycin 100 μg/ml, Gibco) at 37 °C, 5% (v/v) CO_2. When the cells achieved 70–80% confluence, they were exposed to various concentrations of SFN for different times with DMSO (0.1%) as control.

2.3. MTT assay

Cells were seeded into 96-well plates and allowed to grow to approximately 70–80% confluency. After exposure to experimental conditions, MTT (5 mg/ml) was added and incubated with the cells at 37 °C for 1 h. The formazan crystals produced were dissolved in DMSO and the absorbance was determined at test wavelength of 570 nm and background wavelength at 670 nm. Cell viability (%) was determined as [A570nm-A670nm (test)]/[A570nm-A670nm (control)] × 100%; the half-maximal inhibitory concentration (IC_{50}) was calculated with CalcuSyn software Version 2.0 (Biosoft, UK).

2.4. Alkaline comet assay

Cells were seeded into 24-well plates and allowed to grow to approximately 70–80% confluency, then placed in experimental conditions. Cells were then harvested and resuspended in PBS containing 10% DMSO. The alkaline Comet assay procedure was performed as previously described (Liu et al., 2018a). Levels of DNA strand breaks were expressed as tail intensity (% DNA in the Comet tail).

2.5. Annexin V/PI apoptosis assay

HepG2 cells were seeded on 12-well plates at a density of 5×10^4 cells per well and incubated at 37 °C for 48 h. After treatment with 0, 1.25, 2.5, 5, 10, 20 μM SFN for 24 h, cells were exposed to 700 μM H_2O_2 for another 24 h. Medium and PBS used to wash the cell layer were then collected. Cells were trypsinised and added to the collection. After centrifugation at 200*g* for 5 min at 4 °C, the pellets formed were washed with cold PBS before being re-suspended in 1 × binding buffer at a density of 1×10^5/mL according to the instructions from the Annexin V-FITC apoptosis detection kit (eBiosciences, UK). Samples were run on a flow cytometer (Cube 6, Sysmex Partec, Germany). For each sample 10,000 events were collected, and the data were analysed using FlowJo software (Treestar Inc., USA).

2.6. High-performance liquid chromatography (HPLC) analysis of intracellular GSH

Cells were seeded into 6-well plates and allowed to grow to approximately 70–80% confluency, then placed in experimental conditions. Cells were then harvested and suspended in 75 μL PBS containing 5 mM diethylenetriaminepentaacetic acid and 300 μL 50 mM methanesulfonic acid. GSH-containing supernatants were extracted from cells and analysed by HPLC as previous described (Wang et al., 2015b). Briefly, GSH was derivatized using monobrow mobimane (mBBr), the GSH-mBBr adduct was then measured by high-performance liquid chromatography (HPLC) with fluorescence detection. The separation was performed on an ACE-AR C18 reversed phase column (4.6 × 250 mm, 5 μm, HiChrom) a Synergi™ 4 μm Hydro-RP 80 Å LC column (150 × 4.6 mm, Phenomenex) with a mobile phase containing (0.25% acetic acid and 10% methanol in H_2O, pH4) and a flow rate of 1 ml/min. Detection was conducted with excitation wavelength at 385 nm and emission wavelength at 460 nm. The GSH-mBBr adduct peak eluted at 8.9 min and was quantified from a standard curve. The concentration of GSH was expressed as nmol/mg of cellular soluble protein.

2.7. Knockdown of Nrf2 by siRNA

Transfection of siRNA was performed using HiPerFect transfection reagent (Qiagen, West Sussex, UK) according to the manufacturer's protocol. For Comet assay, HepG2 cells were seeded at 0.5–1.5 × 10^5 cells/well of a 24-well plate in 0.5 ml of complete medium, then 30 nM siRNA and 3 μL of HiPerFect transfection reagent were added to 100 μL medium without serum or antibiotics, mixed and incubated for 5–10 min at room temperature to allow the formation of transfection complexes. The complexes were then added drop-wise to each well to give a final siRNA concentration of 5 nM. Cells were cultured for additional 24 h. The Comet assay was then performed as described. For MTT assay, reverse transfection of adherent cells in 96-well plates was used. The MTT assay was performed after 24 h as described.

2.8. Protein extraction and immunoblotting

Cells were seeded into 6-well plates for total protein extraction, or 10 cm dishes for the nuclear protein extraction. After cells reached 70–80% confluence, they were placed in experimental conditions. Cell monolayers were washed twice with ice-cold PBS and lysed with a 6:1 mixture of NP40: proteinase inhibitor (7X stock solution) for whole protein extraction, or with the Nuclear Extract Kit (Active Motif) for nuclear protein extraction. Protein concentration was determined by the Bradford assay.

Protein extracts were loaded onto 10% SDS-polyacrylamide gels. After electrophoresis, proteins were transferred to polyvinylidene difluoride (PVDF) membrane, which was then blocked with 5% fat free milk in PBST (PBS with 0.01% Tween 20) for 1 h, incubated with primary antibody overnight at 4 °C and HRP-conjugated secondary antibody for 1 h. Immunoreactivity was determined by a chemiluminescence detection kit (GE Healthcare, Amersham, UK) and quantified by ImageJ (Schneider et al., 2012).

2.9. Statistics

Data were represented as the mean ± SD (standard deviation). A Student's t-test analysis was performed to determine any statistical difference between two groups. One-way ANOVA with Tukey's *post hoc* analysis was used to estimate associations. A p value < 0.05 was considered statistically significant.

3. Results

3.1. Effect of SFN on cell viability and DNA integrity

The cytotoxicity of SFN was measured by MTT assay so that the appropriate experimental concentrations for further investigation could be established. Both HHL5 and HepG2 cells were cultured in 96-well plates to 70–80% confluence and then treated with SFN (1.25–160 μM) for 24 h. Results indicated that SFN ($\geq$ 20 μM) decreased the metabolic activities of both cell lines in a dose-dependent manner (Fig. 1A). With increasing SFN doses, a decrease of cell confluence and an increase of detached cells and cell debris were observed. The IC_{50} values of SFN were 30.2 and 54.9 μM in HHL5 and HepG2 cells respectively, indicating that HHL5 cells were more susceptible to cytotoxicity from SFN than the hepatoma HepG2 cells. In addition, 1.25 μM SFN treatment increased cell viability in HepG2 cells significantly but not in HHL5 cells ($p < 0.05$).

The genotoxicity of SFN was measured in both cell lines by the Comet assay, using doses of 1.25–20 μM to avoid over-cytotoxicity. Baseline DNA damage (without addition of SFN) in HHL5 and in HepG2 was 7.58 vs 15.94% respectively, represented as background tail intensity (Fig. 1B). The difference may be as a result of the genomic instability of the cancer cells compared to the normal cells (Charames and Bapat, 2003). After 24 h, there was a significant increase in DNA damage from 20 μM SFN treatment in both cell lines, 21.15 and 24.57% in HHL5 and HepG2 respectively; a 2.8-fold increase in DNA damage in HHL5 and 1.5-fold in HepG2 compared to controls. Furthermore, 1.25–10 μM SFN decreased DNA damage in HepG2 cells but not in HHL5 cells.

To reduce the chances of DNA repair processes completely repairing any damage from genotoxic insults, the Comet assay was performed after 30 min exposure to 20, 40, 80 μM SFN treatment in both cell lines (Fig. 1C). Results showed SFN caused DNA damage in a dose-dependent manner in both cell lines, with a 2.8-fold increase at 80 μM SFN treatment in HHL5 and 1.8-fold in HepG2 compared to their corresponding controls. These data are consistent with the cytotoxicity observed between HHL5 and HepG2 cells, suggesting that SFN is more toxic to HHL5 than to HepG2 cells.

3.2. Protective effect of SFN against H_2O_2-induced cell injury

The protective effect of SFN against H_2O_2-induced cell death in both cell lines was determined by MTT assay (Fig. 2A). Cells were pre-treated with SFN (1.25–20 μM) for 24 h then treated with H_2O_2 for another 24 h. The dose of H_2O_2 treatment was at the IC_{50} value in each cell line, i.e. 400 μM and 700 μM in HHL5 and HepG2 respectively (Supplementary Fig. 1A). For HHL5 cells, pre-treatment with 1.25–5 μM SFN alleviated cell death induced by H_2O_2, though pre-treatment with 10 and 20 μM SFN led to more cell death compared to H_2O_2 treatment alone (pre-treated with 0.1% DMSO as control). However, in HepG2 cells, a protective effect was observed from 1.25 to 20 μM SFN pre-treatments in the MTT assays, which was further confirmed using Annexin V/PI double staining. H_2O_2 treatment alone caused significant apoptotic cell death: 5.63% necrotic cells (PI positive) and 30.23% apoptotic cells (Annexin V positive). Pre-treatment with SFN (1.25–20 μM) significantly reduced the cytotoxicity induced by H_2O_2 with an observable increase in the viable cell percentage (double negative) relative to the non-pre-treated cells (Fig. 2B).

The degree by which SFN could protect against H_2O_2-induced DNA damage was then tested by Comet assay (Fig. 2C). Cells were pre-treated with SFN (2.5, 5, 10 μM) for 24 h followed by 60 μM H_2O_2 treatment for 30 min. The dose of H_2O_2 was determined as shown in Supplementary Fig. 1B. In HHL5 cells, only SFN 5 μM pre-treatment provided significant protection against H_2O_2-induced DNA damage; while in HepG2, there was a dose-dependent protective effect from all concentrations of SFN pre-treatment. This result agreed with the changes in p-Chk2 (Thr68) at the protein level observed from Western blotting (Fig. 2D). The phosphorylation of checkpoint kinase 2 (Chk2) indicates its activation, which is well documented as a marker of cellular response to DNA damage (Hirao et al., 2000). H_2O_2 markedly increased the level of p-Chk2 whereas with SFN pre-treatment, p-Chk2 protein decreased in a dose-dependent manner in HepG2 but not in HHL5. These results indicate that SFN significantly reduced the DNA damage caused by H_2O_2 in HepG2 but not in HHL5 cells.

3.3. Effect of SFN on intracellular GSH levels and Nrf2 pathway

The intracellular GSH levels in HHL5 and HepG2 cells were determined by HPLC assay. The basal level of intracellular GSH was 43.9 ± 6.1 nmol/mg in HHL-5 and 60.7 ± 8.5 nmol/mg protein in HepG2 (Supplementary Fig. 2). SFN treatment for 24 h, increased the levels of GSH in a dose dependent manner in both cell lines (Fig. 3A). However, there was a drop of GSH level after 20 μM SFN treatment in HHL5 but not in HepG2 cells, which may represent a toxic effect.

Time courses of the GSH levels in both cell lines were performed following 10 μM SFN treatments (Fig. 3B). Results indicated that SFN caused a biphasic depletion and restoration of GSH in both cell lines. The depletion occurred in HHL5 cells at 3 and 6 h after SFN exposure, where the GSH level decreased to 60 and 72% of control levels respectively. In HepG2 cells, GSH level decreased to 51% at 3 h of SFN

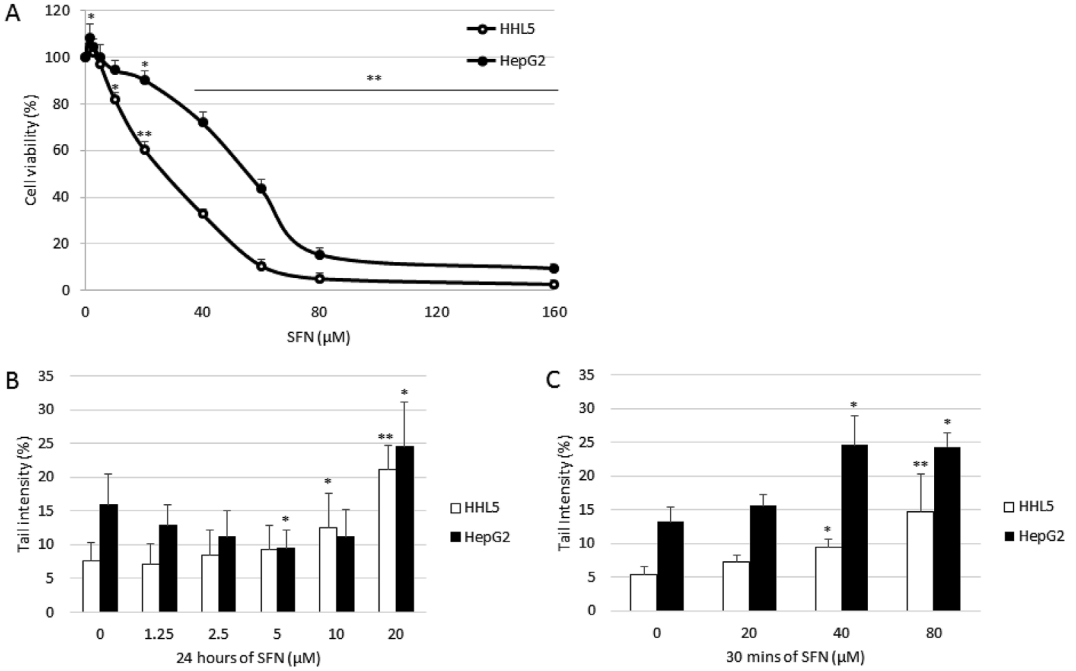

Fig. 1. Effect of SFN on cell viability and genotoxicity in HHL5 and HepG2 cells. (A) Cells were treated with different doses of SFN with DMSO (0.1%) as control for 24 h, then cell viability was determined by MTT assay. Results represent the mean ± SD (n ≥ 5). Lines above the data points indicates significant differences from their corresponding control group. (B) Cells were treated with different doses of SFN with DMSO (0.1%) as control for either 24 h or 30 min (C), then DNA damage was determined by the alkaline Comet assay. Results represent the mean ± SD (n ≥ 3). Statistical significance from the control, *p < 0.05, **p < 0.01.

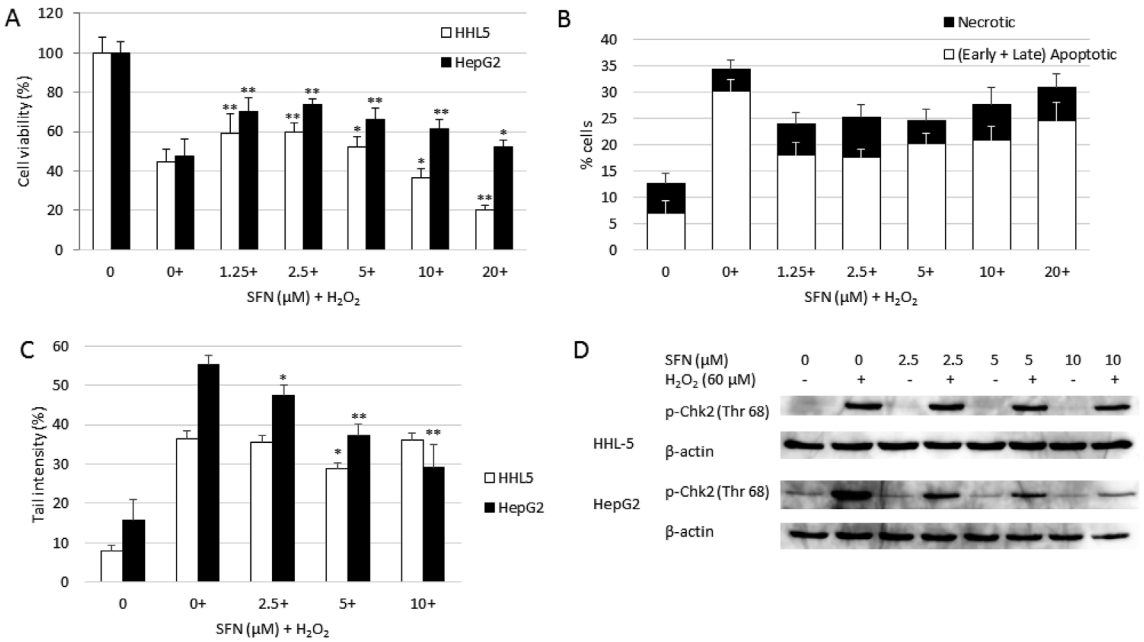

Fig. 2. Protective effect of SFN against H_2O_2-induced cell injury. (A) Cells were pre-treated with different doses of SFN for 24 h and then incubated with H_2O_2 (60 μM) for another 24 h. Cell viability was measured by MTT assay. Results represent the mean ± SD (n ≥ 5). Statistical significance from H_2O_2 control, *p < 0.05, **p < 0.01. (B) HepG2 cells were pre-treated with SFN for 24 h before exposure to H_2O_2 (700 μM) for 24 h, followed by Annexin V/PI staining detected by a flow cytometer. Results represent apoptotic and necrotic cells percentage as mean ± SD (n = 3). (C) Cells were pre-treated with different doses of SFN for 24 h and then incubated with H_2O_2 (60 μM) for another 30 min. DNA damage was measured by Comet assay. Tail intensity were measured for at least 100 Comets per sample. Statistical significance from H_2O_2 control, *p < 0.05, **p < 0.01. (D) The protein level of p-Chk2 in whole cell lysates was detected by Western blot and normalized against β–actin.

treatment but was restored to control levels at 6 h. At 24 h, the GSH levels were increased around 2-fold of controls in both cell lines. These results were in accordance with those of Kim and coworkers (Kim et al., 2003) who showed early down regulation of GSH between 0 and 4 h and up regulation between 4 and 24 h in HepG2-C8 cells.

Since Nrf2 translocation to the nucleus is one of the key events required in the regulation of the Nrf2-Keap1-ARE signalling pathway, it is important to determine the time- and dose-response of SFN on this translocation. Here the time and dose courses of activation Nrf2 by SFN were tested in both cell lines. Untreated HHL5 and HepG2 cells had low

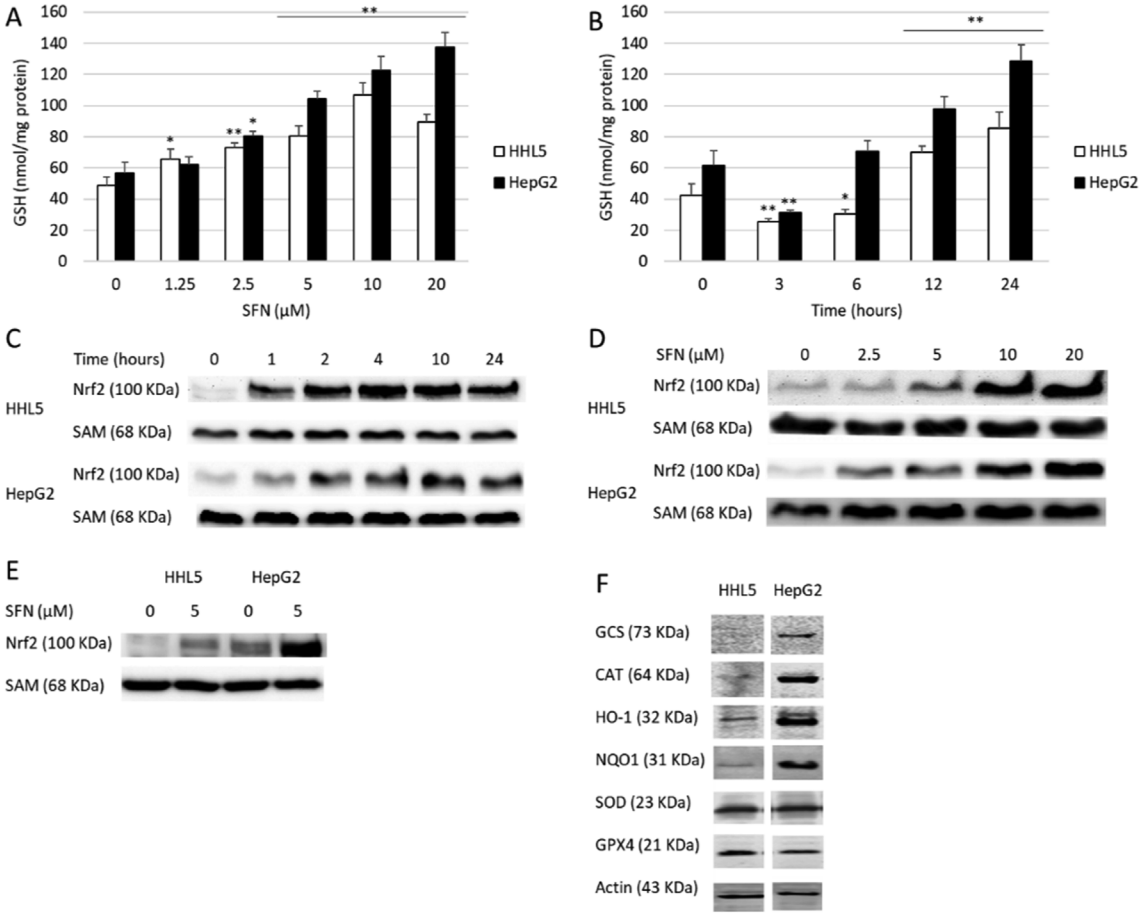

Fig. 3. Effect of SFN on intracellular GSH levels and Nrf2 activation in HHL5 and HepG2 cells. (A) Cells were treated with different doses of SFN with DMSO (0.1%) as control for 24 h, or (B) cells were treated with 10 μM SFN for 0, 3, 6, 12, 24 h. The intracellular GSH level was measured by HPLC. Results represent the mean ± SD (n = 3). Statistical significance from control, *$p < 0.05$, **$p < 0.01$. Nuclear protein was extracted from cells treated with (C) 10 μM SFN from 0 to 24 h, (D) SFN from 0 to 20 μM for 4 h, or (E) SFN 5 μM or DMSO (0.1%) for 4 h, and Nrf2 was detected by Western blotting. RNA-binding protein SAM was used as a loading control. (F) The whole protein levels of GCS, CAT, SOD1, NQO1, SOD and GPX4 were detected by Western blotting using both cell lines. β-actin was used as a loading control.

Nrf2 levels in the nucleus consistent with the continuous degradation of Nrf2 under homeostasis. Upon SFN treatment, a prompt increase of Nrf2 appeared after 1 h in both cell lines (Fig. 3), suggesting the liberation of Nrf2 from Keap1 suppression and subsequent Nrf2 nuclear translocation. The nuclear accumulation of Nrf2 plateaued after 2 h and remained steady for 24 h. The dose response from 4 h SFN treatment in HHL5 cells is in agreement with previous studies (Li et al., 2012b). In HepG2, SFN at 2.5–20 μM also induced significant and dose-dependent translocation of Nrf2 into the nucleus. Comparing the basal levels of nuclear Nrf2 in these two cell lines, HepG2 showed a 3.3-fold higher basal level than HHL5. Moreover, SFN at 5 μM (4 h) induced 2.9- and 6.2-fold increase of Nrf2 protein level in HHL5 and HepG2 cells respectively. As shown in Fig. 3F, GCS was 9.8-fold higher in HepG2 cells than that in HHL5 cells, which was consistent with the basal level of GSH being higher in HepG2 cells compared to HHL5 cells. Other Nrf2-driven enzymes such as CAT, SOD1 and NQO1 were all found significantly higher in HepG2 cells than that of HHL5 cells were significantly higher in HepG2 cells compared to HHL5 cells, and that may explain the stronger ROS scavenging capability of HepG2 cells we observed in Supplementary Fig. 1A.

3.4. The role of Nrf2 and GSH in cytotoxic and cytoprotective effects of SFN

Since higher basal levels of Nrf2 and GSH were observed in HepG2 cells compared to those in HHL5 cells, their role in the cytotoxic effect of SFN was investigated further. BSO, a specific inhibitor of γ-GCS, was used to decrease GSH levels. The inhibition efficiency of BSO on the intracellular GSH level was characterized using HPLC (Supplementary Fig. 3). BSO (50 μM) was used in the co-treatment with SFN as it showed 60–80% reduction in the GSH level and abolished the SFN-induced GSH rise. Nrf2 knockdown was achieved by siRNA transfection. The siRNA knockdown efficiency of Nrf2 was measured using Western blot analysis as previous described (Liu et al., 2018b).

After 24 h treatment with 50 μM BSO, the cell viability of HepG2 cells was still high at 97.9% (Fig. 4A). SFN treatment at 60 μM decreased HepG2 cell viability to 47.6%, which agreed with previous data; while co-treatment with BSO reduced the cell viability further to 25.7%. Furthermore, in control (Allstar transfected) cells, SFN (60 μM) decreased cell viability to 49.5% of control (0.1% DMSO); while in siNrf2 transfected cells, SFN decreased cell viability to 15.3% of controls. These data indicate clearly that reducing Nrf2 and GSH levels in HepG2 cells increased susceptibility to SFN toxicity.

To investigate whether Nrf2 is the main gene responsible for the cytoprotective effect of SFN against H_2O_2-induced cell death in HepG2 cells, cells were transfected with siNrf2 (or Allstar as negative control), pre-treated with 5 μM SFN for 24 h followed by H_2O_2 insult for another 24 h. Nrf2 knockdown enhanced the cytotoxicity of H_2O_2, i.e. cell viability was 47.6, 38.0 and 24.6% in the non-transfected, Allstar transfected and siNrf2 transfected cells respectively (Fig. 4B). 5 μM SFN decreased the cytotoxicity of H_2O_2 in non-transfected and Allstar

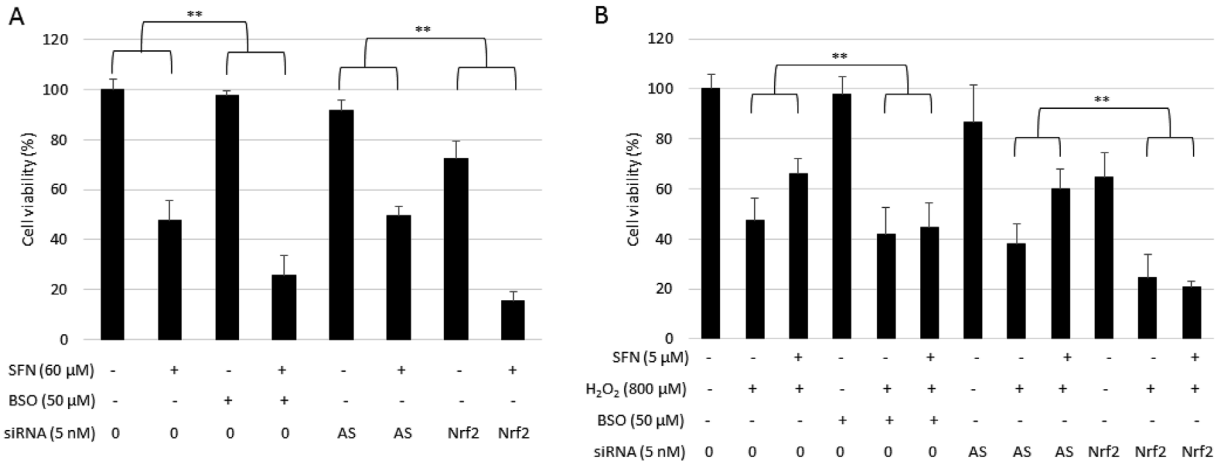

Fig. 4. Effect of GSH inhibition and Nrf2 knockdown on SFN cytotoxic and cytoprotective effects in HepG2 cells. Allstars (AS) was used as a negative control. (A) Cells were incubated with 60 μM SFN or DMSO (0.1%) with or without BSO (50 μM) for 24 h. (B) Cells were incubated with 5 μM SFN or DMSO (0.1%) with or without BSO (50 μM) for 24 h, followed by exposure to 800 μM H_2O_2 for another 24 h. Cell viability was measured by MTT assay, results represent the mean ± SD ($n \geq 5$). Within each set of indicated columns, SFN treated groups were normalized against the mean of corresponding control groups. A student's t-test was then performed to determine any statistical difference between two groups. **$p < 0.01$ between the indicated groups.

negative control cells, while the protective effect from SFN was abolished upon Nrf2 knockdown. The involvement of GSH in the SFN cytoprotective effect was also studied. Co-treatment with BSO and 5 μM SFN showed no protective effect against H_2O_2. Therefore, it can be concluded that the Nrf2/GSH signalling pathway plays an essential role in the protective effect of SFN against H_2O_2 challenges.

4. Discussion

The epidemiological evidence with respect to the consumption of dietary isothiocyanates as chemopreventive agents against cancer has been inconsistent. For example, results from a randomized, placebo-controlled trial in Qidong (China) indicated that intake of 400 μM glucoraphanin, the precursor of SFN, for 2 weeks altered the disposition of aflatoxin and phenanthrene in 200 healthy participants, both of which are known to contribute to the high risk of hepatocellular carcinoma in that region (Kensler et al., 2005). On the other hand, no association between urinary isothiocyantes exposure and liver cancer risk was found in a nested case-control study including Chinese men and women (Wu et al., 2014). Consumption of cruciferous vegetables, at least one portion (around 125 g) per week, also showed no significant association with liver cancer risk reduction in data from case-control studies conducted in Italy and Switzerland (Bosetti et al., 2012).

An ideal chemopreventive agent should only have a minimal effect on normal cells but a strong inhibitory effect on cell proliferation and carcinogenic pathways in cancer cells. While there are many studies on both protective and cytotoxic effects of SFN, there is little data comparing its effect on normal cells with cancer cells. The study presented here is the first to compare the effects of SFN on immortalised hepatocytes (HHL5) versus the hepatoma cell line HepG2.

SFN showed stronger cytotoxicity and genotoxicity in HHL5 than in HepG2. At 24 h, 10 μM SFN started to inhibit cell viability and induce DNA damage in HHL5 while in HepG2 only concentrations above 20 μM SFN had a significant cytotoxic and genotoxic effect. Since the cytotoxic effects of SFN and H_2O_2 have been linked to the disruption of the redox status of the cells (Sestili and Fimognari, 2015; Sies, 2014), the different sensitivities towards oxidative stress between these two cell lines observed is possibly due to differences in their Nrf2-driven enzymes and GSH response systems. Indeed, results showed that HepG2 cells had higher basal levels of intracellular GSH, nuclear Nrf2 and some of the phase II enzyme such as CAT, HO-1, NQO1, than HHL5 cells, which could indicate they have an enhanced defence system against ROS compared to HHL5 cells. Targeting tumor detoxification enzymes has been considered as an attractive strategy for selective antitumor therapy (Bauer, 2012; Oh and Park, 2015; Chau, 2015).

More interestingly, SFN increased nuclear Nrf2 levels and intracellular GSH levels in both cell lines but with slightly different patterns. Short term SFN exposure (3–6 h) of HHL5 cells depleted intracellular GSH for longer and exhibited lower induction of Nrf2 nuclear accumulation compared to HepG2 cells. These findings indicate that SFN may exhibit strong pro-survival effects in HepG2 cells, which is in line with the results shown in Fig. 2. Pre-treatment for 24 h with SFN provided protection against H_2O_2-induced cell injury in both cell lines. However, in HHL5 cells, SFN at high doses (10–20 μM) failed to show a protective effect against H_2O_2-induced cell death and DNA damage.

Nrf2 is generally considered as a primary defence mechanism of the cell and a major regulator of cell survival. Nrf2 deficient mice are more susceptible to carcinogenesis (Yokoo et al., 2016; Cheung et al., 2014). Many have reported the chemopreventive effect of Nrf2 in cancer (Lu et al., 2016; Russo et al., 2018; Krajka-Kuźniak et al., 2017). However, the results of the present study indicate that in HepG2, the inhibition of Nrf2/GSH increased SFN cytotoxicity and decreased its cytoprotective effect against H_2O_2 challenge, i.e., both Nrf2 and GSH substantially contributed to the preservation of cell integrity under conditions of SFN and H_2O_2 treatment in HepG2 cells. The knockdown of Nrf2 increased cell death even further in both cell lines compared to GSH inhibition, indicating that more Nrf2 targets might be involved. Essentially, Nrf2 protects not only normal cells but also transforming/cancer cells. With increasing evidence suggesting that Nrf2 is upregulated in cancer cells or resistance strains (Taguchi et al., 2011; Menegon et al., 2016), and that it contributes to the aggressive cancer phenotype (Kansanen et al., 2013), it has become more important to rationalise the usage of Nrf2 inhibitors vs activators. In this study, HepG2 cells were able to take advantage of the SFN-induced protective effects, and better resist SFN-induced disruptions than HHL5 cells, indicating a potential risk of chemo-resistance of using SFN for chemoprevention. More rigorous dose-response comparisons of efficacy versus toxicity need to be performed *in vivo* with consideration of the differences between normal and cancer cells.

In conclusion, human hepatoma HepG2 cells were more resistant to SFN exposure compared to immortalised heptocyte HHL5 cells, which may be due to their intrinsic high expression of Nrf2/GSH. SFN exhibited strong cytoprotective effects due to the activation of Nrf2 and the induction of GSH in both cell lines. Although *in vitro* studies do not necessarily predict *in vivo* outcomes, these findings raise the question

that SFN may induce pro-survival effects in cancer cells. Therefore, a combination of inhibition Nrf2/GSH and chemopreventive agents may be a better strategy in cancer management since multiple targeted approaches can improve the efficacy of anti-cancer drugs and minimise the adverse effects toward normal cells.

Conflicts of interest

None.

Acknowledgements

The authors wish to thank Chris Washbourne for help in using the HPLC facilities, Dr Andrew Smith, Professor Michael Wormstone and Human Research Trust for setting up the Comet assay, Dr A. Patel, Medical Research Council (MRC) Virology Unit (Glasgow, UK) for supplied the HHL5 cells. We also thank Mr Jim Bacon for helpful discussion during the preparation of this manuscript.

Appendix A. Supplementary data

Supplementary data to this article can be found online at https://doi.org/10.1016/j.fct.2019.03.050.

Transparency document

Transparency document related to this article can be found online at https://doi.org/10.1016/j.fct.2019.03.050.

Financial Support

This work was supported by an International PhD Studentship (University of East Anglia, UK) to P. Liu, and in part, an award from the Cancer Prevention Research Trust (UK) to Y. Bao. We also would like to thank The Humane Research Trust and the John and Pamela Salter Charitable Trust for their support of the equipment and software for the Comet Assay.

References

Agyeman, A.S., et al., 2012. Transcriptomic and proteomic profiling of KEAP1 disrupted and sulforaphane-treated human breast epithelial cells reveals common expression profiles. Breast Canc. Res. Treat. 132, 175–187.
Baird, L., Dinkova-Kostova, A.T., 2011. The cytoprotective role of the Keap1-Nrf2 pathway. Arch. Toxicol. 85, 241–272.
Bauer, G., 2012. Tumor cell-protective catalase as a novel target for rational therapeutic approaches based on specific intercellular ROS signaling. Anticancer Res. 32, 2599–2624.
Beaver, L.M., et al., 2014. Transcriptome analysis reveals a dynamic and differential transcriptional response to sulforaphane in normal and prostate cancer cells and suggests a role for Sp1 in chemoprevention. Mol. Nutr. Food Res. 58, 2001–2013.
Bosetti, C., et al., 2012. Cruciferous vegetables and cancer risk in a network of case-control studies. Ann. Oncol. 23, 2198–2203.
Byun, S., et al., 2016. Sulforaphene suppresses growth of colon cancer-derived tumors via induction of glutathione depletion and microtubule depolymerization. Mol. Nutr. Food Res. 60, 1068–1078.
Charames, G.S., Bapat, B., 2003. Genomic instability and cancer. J. Mol. Cell Biol. 3, 1–3.
Chau, L.Y., 2015. Heme oxygenase-1: emerging target of cancer therapy. J. Biomed. Sci. 22.
Cheung, K.L., et al., 2014. Nrf2 knockout enhances intestinal tumorigenesis in Apcmin/+ mice due to attenuation of anti-oxidative stress pathway while potentiates inflammation. Mol. Carcinog. 53, 77–84.
Chung, Y.K., et al., 2015. Sulforaphane down-regulates SKP2 to stabilize $p27^{KIP1}$ for inducing antiproliferation in human colon adenocarcinoma cells. J. Biosci. Bioeng. 119, 35–42.
Clarke, J.D., Hsu, A., Yu, Z., Dashwood, R.H., Ho, E., 2011. Differential effects of sulforaphane on histone deacetylases, cell cycle arrest and apoptosis in normal prostate cells versus hyperplastic and cancerous prostate cells. Mol. Nutr. Food Res. 55, 999–1009.
Clayton, R.F., et al., 2005. Liver cell lines for the study of hepatocyte functions and immunological response. Liver Int. 25, 389–402.
Constantinescu, S., et al., 2014. Transcriptomic responses of cancerous and noncancerous human colon cells to sulforaphane and selenium. Chem. Res. Toxicol. 27, 377–386.
Fimognari, C., et al., 2004. Isothiocyanates as novel cytotoxic and cytostatic agents: molecular pathway on human transformed and non-transformed cells. In: Biochemical Pharmacology, vol. 68. pp. 1133–1138.
Gamet-Payrastre, L., et al., 2000. Sulforaphane, a naturally occurring isothiocyanate, induces cell cycle arrest and apoptosis in HT29 human colon cancer cells. Cancer Res. 60, 1426–1433.
Herz, C., et al., 2014. The isothiocyanate erucin abrogates telomerase in hepatocellular carcinoma cells in vitro and in an orthotopic xenograft tumour model of HCC. J. Cell Mol. Med. 18, 2393–2403.
Hirao, A., et al., 2000. DNA damage-induced activation of p53 by the checkpoint kinase Chk2. Science 287, 1824–1827 80-.
Hu, C., Eggler, A.L., Mesecar, A.D., Van Breemen, R.B., 2011. Modification of Keap1 cysteine residues by sulforaphane. Chem. Res. Toxicol. 24, 515–521.
Jackson, S.J.T., Singletary, K.W., 2004. Sulforaphane: a naturally occurring mammary carcinoma mitotic inhibitor, which disrupts tubulin polymerization. Carcinogenesis 25, 219–227.
Jackson, S.J.T., Singletary, K.W., Venema, R.C., 2007. Sulforaphane suppresses angiogenesis and disrupts endothelial mitotic progression and microtubule polymerization. Vasc. Pharmacol. 46, 77–84.
Kansanen, E., Kuosmanen, S.M., Leinonen, H., Levonenn, A.L., 2013. The Keap1-Nrf2 pathway: mechanisms of activation and dysregulation in cancer. Redox Biol 1, 45–49.
Katoh, Y., et al., 2005. Evolutionary conserved N-terminal domain of Nrf2 is essential for the Keap1-mediated degradation of the protein by proteasome. Arch. Biochem. Biophys. 433, 342–350.
Kensler, T.W., et al., 2005. Effects of glucosinolate-rich broccoli sprouts on urinary levels of aflatoxin-DNA adducts and phenanthrene tetraols in a randomized clinical trial in He Zuo Township, Qidong, People's Republic of China. Cancer Epidemiol. Biomark. Prev. 14, 2605–2613.
Kim, B.R., et al., 2003. Effects of glutathione on antioxidant response element-mediated gene expression and apoptosis elicited by sulforaphane. Cancer Res. 63, 7520–7525.
Krajka-Kuźniak, V., Paluszczak, J., Baer-Dubowska, W., 2017. The Nrf2-ARE signaling pathway: an update on its regulation and possible role in cancer prevention and treatment. Pharmacol. Rep. 69, 393–402.
Li, Y., et al., 2012a. Sulforaphane inhibits pancreatic cancer through disrupting Hsp90-p50Cdc37 complex and direct interactions with amino acids residues of Hsp90. J. Nutr. Biochem. 23, 1617–1626.
Li, D., et al., 2012b. Synergy between sulforaphane and selenium in the up-regulation of thioredoxin reductase and protection against hydrogen peroxide-induced cell death in human hepatocytes. Food Chem. 133, 300–307.
Liu, H., et al., 2017. Sulforaphane promotes ER stress, autophagy, and cell death: implications for cataract surgery. J. Mol. Med. 95, 553–564.
Liu, P., et al., 2018a. Chemopreventive activities of sulforaphane and its metabolites in human hepatoma HepG2 cells. Nutrients 10, 585.
Liu, P., et al., 2018b. Anti-cancer activities of allyl isothiocyanate and its conjugated silicon quantum dots. Sci. Rep. 8.
Lu, S.C., 2009. Regulation of glutathione synthesis. Mol. Aspect. Med. 30, 42–59.
Lu, M.C., Ji, J.A., Jiang, Z.Y., You, Q.D., 2016. The keap1–Nrf2–ARE pathway as a potential preventive and therapeutic target: an update. Med. Res. Rev. 36, 924–963.
Lubelska, K., et al., 2016. Sulforaphane regulates NFE2L2/Nrf2-dependent Xenobiotic metabolism phase II and phase III enzymes differently in human colorectal cancer and untransformed epithelial colon cells. Nutr. Canc. 68, 1338–1348.
Menegon, S., Columbano, A., Giordano, S., 2016. The dual roles of NRF2 in cancer. Trends Mol. Med. 22, 578–593.
Misiewicz, I., Skupinska, K., Kasprzycka-Guttman, T., 2007. Differential response of human healthy lymphoblastoid and CCRF-SB leukemia cells to sulforaphane and its two analogues: 2-oxohexyl isothiocyanate and alyssin. Pharmacol. Rep. 59, 80–87.
Mitsuishi, Y., et al., 2012. Nrf2 redirects glucose and glutamine into anabolic pathways in metabolic reprogramming. Cancer Cell 22, 66–79.
Moon, D.O., et al., 2010. Sulforaphane decreases viability and telomerase activity in hepatocellular carcinoma Hep3B cells through the reactive oxygen species-dependent pathway. Cancer Lett. 295, 260–266.
Nakagawa, K., et al., 2006. Evaporative light-scattering analysis of sulforaphane in broccoli samples: quality of broccoli products regarding sulforaphane contents. J. Agric. Food Chem. 54, 2479–2483.
Negrette-Guzman, M., et al., 2017. Sulforaphane induces differential modulation of mitochondrial biogenesis and dynamics in normal cells and tumor cells. Food Chem. Toxicol. 100, 90–102.
Oh, E.T., Park, H.J., 2015. Implications of NQO1 in cancer therapy. BMB Reports 48, 609–617.
Park, H.S., et al., 2014. Sulforaphane induces reactive oxygen species-mediated mitotic arrest and subsequent apoptosis in human bladder cancer 5637 cells. Food Chem. Toxicol. 64, 157–165.
Pham, N.A., et al., 2004. The dietary isothiocyanate sulforaphane targets pathways of apoptosis, cell cycle arrest, and oxidative stress in human pancreatic cancer cells and inhibits tumor growth in severe combined immunodeficient mice. Mol. Canc. Therapeut. 3, 1239–1248.
Pledgie-Tracy, A., Sobolewski, M.D., Davidson, N.E., 2007. Sulforaphane induces cell type-specific apoptosis in human breast cancer cell lines. Mol. Canc. Therapeut. 6, 1013–1021.
Russo, M., et al., 2018. Nrf2 targeting by sulforaphane: a potential therapy for cancer treatment. Crit. Rev. Food Sci. Nutr. 58, 1391–1405.
Schneider, C.A., Rasband, W.S., Eliceiri, K.W., 2012. NIH Image to ImageJ: 25 years of image analysis. Nat. Methods 9, 671–675.
Sestili, P., Fimognari, C., 2015. Cytotoxic and antitumor activity of sulforaphane: the role of reactive oxygen species. BioMed Res. Int. 1–9 (2015).
Sestili, P., et al., 2010. Sulforaphane induces DNA single strand breaks in cultured human

cells. Mutat. Res. 689, 65–73.
Sies, H., 2014. Role of metabolic H2O2 generation: redox signaling and oxidative stress. J. Biol. Chem. 289, 8735–8741.
Suppipat, K., Park, C.S., Shen, Y., Zhu, X., Lacorazza, H.D., 2012. Sulforaphane induces cell cycle arrest and apoptosis in acute lymphoblastic leukemia cells. PLoS One 7.
Taguchi, K., Motohashi, H., Yamamoto, M., 2011. Molecular mechanisms of the Keap1-Nrf2 pathway in stress response and cancer evolution. Genes Cells 16, 123–140.
Tang, L., Zhang, Y., 2005. Mitochondria are the primary target in isothiocyanate-induced apoptosis in human bladder cancer cells. Mol. Canc. Therapeut. 4, 1250–1259.
Thimmulappa, R.K., et al., 2002. Identification of Nrf2-regulated genes induced by the chemopreventive agent sulforaphane by oligonucleotide microarray. Cancer Res. 62, 5196–5203.
Townsend, D.M., Tew, K.D., Tapiero, H., 2003. The importance of glutathione in human disease. Biomed. Pharmacother. 57, 145–155.
Wang, Y., et al., 2015a. Synergy between sulforaphane and selenium in protection against oxidative damage in colonic CCD841 cells. Nutr. Res. 35, 610–617.
Wang, W., et al., 2015b. Sulforaphane protects the liver against CdSe quantum dot-induced cytotoxicity. PLoS One 10, e0138771.
Wong, C.P., et al., 2014. Effects of sulforaphane and 3,3′-diindolylmethane on genome-wide promoter methylation in normal prostate epithelial cells and prostate cancer cells. PLoS One 9.
Wu, Q.J., et al., 2014. Urinary isothiocyanates level and liver cancer risk: a nested case-control study in Shanghai, China. Nutr. Canc. 66, 1023–1029.
Yokoo, Y., et al., 2016. Effects of Nrf2 silencing on oxidative stress-associated intestinal carcinogenesis in mice. Cancer Med 5, 1228–1238.
Zeng, H., Trujillo, O.N., Moyer, M.P., Botnen, J.H., 2013. Prolonged sulforaphane treatment activates survival signaling in nontumorigenic NCM460 colon cells but apoptotic signaling in tumorigenic HCT116 colon cells. Nutr. Canc. 15, 2379–2381.
Zhang, Y., Talalay, P., Cho, C.G., Posner, G.H., 1992. A major inducer of anticarcinogenic protective enzymes from broccoli: isolation and elucidation of structure. Proc. Natl. Acad. Sci. U. S. A 89, 2399–2403.
Zhang, D.D., et al., 2005. Ubiquitination of Keap1, a BTB-Kelch substrate adaptor protein for Cul3, targets Keap1 for degradation by a proteasome-independent pathway. J. Biol. Chem. 280, 30091–30099.